PSO Tuning of a Second Order Sliding Mode Controller to Adjust Active Standard Power Levels on a Single-Phase Voltage Source Inverter

Óscar Gonzales-Zurita
Institute for Energy Engineering
Universitat Politècnica de València
Valencia, Spain
ogonzal@doctor.upv.es

Jean-Michel Clairand
Facultad de Ingeniería y Ciencias Aplicadas
Universidad de las Américas - Ecuador
Quito, Ecuador
jean.clairand@udla.edu.ec

Guillermo Escrivá-Escrivá
Institute for Energy Engineering
Universitat Politècnica de València
Valencia, Spain
guieses@die.upv.es

***Abstract*—Electricity management in non-conventional energy systems requires advanced control algorithms to produce and distribute electricity efficiently. Various countries worldwide have promoted policies to manage electricity from power inverters under typical voltage, current, and power values. This paper proposes a DQ control for active power regulation on a single-phase voltage source inverter (SPVSI) using a Second Order Sliding Mode Control (SMC-2). The SMC-2 tunning is performed by a metaheuristics algorithm like the Particle Swarm Optimization (PSO) to adjust the SMC-2 parameters. PSO appropriately tuns the SMC-2 through MATLAB, where the results showed lower Integral of Absolute Error value (IAE) and Integral of Square Error value (ISE) as performance indexes.**

***Index Terms*—Particle Swarm Optimization (PSO), Second-order Sliding Mode Controller (SMC-2), Single-phase Voltage Source Inverter (SPVSI), Integral of Absolute Error (IAE), Integral of Square Error (ISE).**

I. Introduction

Currently, society seeks an alternative to global change effects promoting the use of renewable energy. Distributed generation (DG) systems produce electricity from various small installations located near the demand side. DG generates electrical energy from diverse resources like the sun, the wind, the sea waves, the mechanical movement of rotating machines, conventional fuels, among others [1], [2].

The voltage source inverter (VSI) is one essential component of an inverter-based DG; the VSI constitutes a power electronic converter that transforms the direct current (DC) into the alternate current (AC). For instance, some renewable energy applications use photovoltaic systems that produce DC current; the VSI transforms this energy into AC current for most AC appliances [3]. The closed-loop control of VSI represents an emerging area of research due to the massive implementation of DG in the last years. Authors like [4] realized that some controllers on VSI can experience disadvantages, for example, the PI regulator in the DQ reference frame. Therefore, they proposed a hybrid fuzzy-PI to improve control law capabilities by making the algorithm more robust. However, PI controllers suffer certain disadvantages in some operating points that cause oscillations due to the windup effect. Also, errors in steady-state can be increased when the plant's dynamics reach non-linear regions. PI controllers have satisfactory performance in a region near the operation point. However, if exist a big change in the reference, the control actions might miss precision. These great changes represent a challenge for any control design because exist scenarios where the linearity, controlability and stability are lost. Nevertheless, [5] implemented a control law in DQ coordinates for a single-phase VSI. The DQ coordinates were conceived for three-phase systems. To apply a DQ reference frame in a single-phase system is a bit complicated because an alpha-beta (AB) reference frame is needed first. Therefore, the authors obtained the current value through the capacitor as part of the alpha component. This technique can generate problems in the stability of the current controller because the capacitor is influenced by the high-frequency switching of the VSI that produces current harmonic components. Other authors like [6] developed an optimal control algorithm like Model Predictive Control (MPC) to regulate the current on a Microgrid-Connected PWM Inverter. The MPC established predictions based on the model of the process to anticipate the control actions. Oppositely, if the model of the inverter is inaccurate, the control actions are not adequately calculated. In this sense, this work implements a robust algorithm like a second-order Sliding Mode Control (SMC-2) that approaches the problem of stability under different operating points of operation. The controller is implemented using DQ coordinates to establish independent control of active power. Power references are placed with a ramp value established by policies in inverter-grid applications. The Particle Swarm Optimization (PSO) algorithm is used to get the SMC-2 parameters to get optimal response.

This paper is organized as follows. Section II presents a background of the SPVSI and the algorithms used in this work. Section III describes the methodology developed to obtain the control law. Section IV presents the main results and discussion of this work. Finally, Section V is devoted to conclude this paper.

II. Single-Phase Voltage Source Inverter background and control

A. Modelling the Single-Phase Voltage Source Inverter

A single-phase voltage source inverter (SPVSI) generates AC current from a fixed voltage in DC current. The most widely SPVSI topology used is the H-bridge because the maximum output voltage levels are equal to the input DC bus. This structure includes four power switches coupled in two branches. The switches change states according to the modulation technique of the control circuit. To reduce the harmonic content of the output voltage, SPWM modulation is employed. This technique eliminates the high-order harmonic components by including a filter at the output terminals of the VSI. The SPWM changes the states of the power switches to generate an alternating voltage as noted in Table I.

TABLE I
Switching states of power electronic devices on SPVSI.

S_1	S_2	S_3	S_4	V_{SPVSI}
1	0	0	1	V_{DC}
0	1	1	0	$-V_{DC}$
1	1	0	0	0
0	0	1	1	0

The output voltage at the SPVSI (V_{SPVSI}) is generated from values of 0, V_{DC} and $-V_{DC}$ to produce alternating voltage. The standard closed-loop scheme for VSI is seen in Fig. 1.

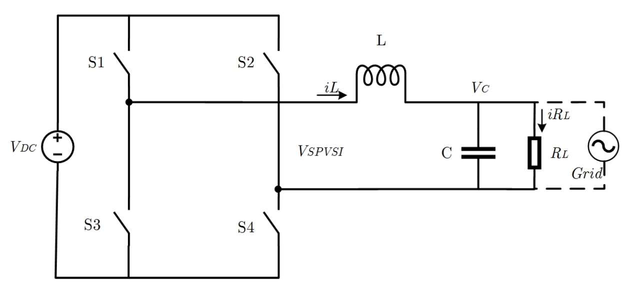

Fig. 1. SPVSI scheme for closed-loop control.

The LC component is a low-pass filter that eliminates high-order harmonics. The cut-off frequency is set to the standard frequency in every country. The equations that represent the dynamics of SPVSI are presented as follows:

$$\frac{di_L}{dt} = \frac{1}{L} \cdot [S_{ab}V_{DC} - R_L \cdot i_R L] \tag{1}$$

$$\frac{dV_c}{dt} = \frac{1}{C} \cdot \left[i_L - \frac{V_c}{R_L} \right] \tag{2}$$

$$i_{DC} = s_{ab} \cdot \ i_c \tag{3}$$

B. DQ Reference Frame

The DQ reference frame represents DC equivalent expressions for non-stationary vectors. Complex mathematical equations can be used in a simpler way to design closed.loop controllers. The DQ reference frame is also called as Park transformation, and it is represented as a matrix T like:

$$T = \begin{bmatrix} \cos\theta & \sin\theta \\ -\sin\theta & \cos\theta \end{bmatrix} \tag{4}$$

The DQ transformation takes the signals in the AB reference frame. Since the SPVSI has one phase, an orthogonal component is needed to perform the DQ transformation. The first-order low-pass filter is used twice to obtain the 90° difference between A and B signals.

$$v_a = \frac{1}{\tau s + 1} v_b \tag{5}$$

The B component is chosen from the SPVSI model. The component is the grid's voltage for voltage, and the current component is the SPVSI's current. The time constant τ is set based on the grid's voltage.

The transformation is applied to voltage and current values from the VSI. The current controller uses the current of the DQ coordinate frame. These expressions are seen as:

$$u_d = L\frac{di_d}{dt} + \omega \ Li_q + R_L i_d + v_d \tag{6}$$

$$u_q = L\frac{di_q}{dt} - \omega \ Li_d + R_L i_q + v_q \tag{7}$$

C. Second-Order Sliding Mode Controller

The formulation of any control algorithm takes the basic model of a process like:

$$\dot{x} = f(t, x, u), s = s(t, x) \in \mathbb{R}, u = U(t, x) \in \mathbb{R} \tag{8}$$

Let the system be expressed as follows:

$$\dot{x} = f(t, x, u) \tag{9}$$

The sliding surface and control law are represented as:

$$s = s(t, x) \in \mathbb{R}, u = U(t, x) \in \mathbb{R} \tag{10}$$

An SMC-2 avoids the chattering effect that generates a high-frequency control law that electromechanical systems cannot achieve. This approach was proposed by [7], where the control signal dynamics remain in a small vicinity on a discontinuous surface. As a result, the main properties of the plant under the regulation are maintained. This approach was analyzed by Filippov's sense where the SMC-2 on a discontinuity set of a dynamic system. In this sense, the high sliding order comes from several continuous derivates of the sliding surface as seen in:

$$s = \dot{s} = \ddot{s} = \ldots = s^{(r-1)} = 0 \tag{11}$$

The suitable controller for SMC-2 used in this work is known as super-twisting algorithm [8] and it is described as seen in Fig. 2.

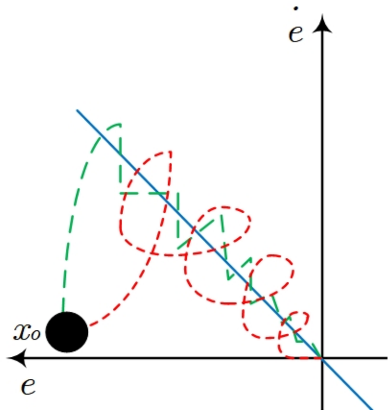

Fig. 2. Differences between conventional SMC and HOSMC.

There are two terms on the super-twisting control law. The first one is defined by its continuous-time derivative, and the second represents a continuous function of the sliding variable applied.

$$u(t) = u_1(t) + u_2(t) \tag{12}$$

$$u = -\lambda |s|^{\rho} sign\,(s) + u_1 \tag{13}$$

$$\dot{u}_1 = -W sign\,(s) \tag{14}$$

Where W, λ, and ρ represent the gains on the SMC-2 algorithm. An advantage of the super-twisting method is that it does not need the derivate of the sliding variable $\dot{s}$ that is required for other SMC alternatives.

D. Particle Swarm Optimization (PSO) [9]

PSO algorithm is a metaheuristics process developed by Kennedy and Eberhart [10] to simulate the behavior of biological systems. The algorithm is contrasted with a searching process performed by biological groups. Every agent in the group collaborates with its neighbors to find a specific objective. The objective is in the space of D solutions. At first, N particles are distributed in the solution space as random points. Each particle X_i represents a point with coordinates:

$$X_i = (x_{i1}, x_{i2}, \cdots, x_{iD}) \tag{15}$$

Each element moves with a velocity V_i with coordinates:

$$V_i = (v_{i1}, v_{i2}, \cdots, v_{iD}) \tag{16}$$

Each particle updates its position and velocity to accomplish the optimal value. The best position is updated as:

$$X_i = X_i + V_i \tag{17}$$

TABLE II
PSEUDOCODE FOR PSO/SMC-2 TUNING.

Setting of N-particles population;
Initialization of position and velocity of each particle for λ and W;
For each iteration:
Fitness value calculation to minimize error tracking;
Update personal and global best;
Until meeting stopping criterion;
Optimal output value;

$$V_i = \omega\ V_i + c_1 r_1 \left(p_{\text{besti}-\ x_i}\right) + c_2 r_2 \left(g_{\text{best}}\ - X_i\right) \tag{18}$$

Where p_{besti} is the best position of each particle in the set, g_{best} is the best global position of a particle in the swarm, c_1 and c_2 represent learning factors that are constants, r_1 and r_2 random numbers between 0 to 1 that tune the algorithm, and ω the inertial weight commonly represented by values between 0.1 to 0.9.

III. METHODOLOGY

A. Control law design

The sliding surface is chosen as a PI function like:

$$s = K_p e + K_i \int e \tag{19}$$

To generate a robust control action, the Lyapunov [11] stability criterion is utilized:

$$s(x)\dot{s}(x) < 0 \tag{20}$$

Replacing the sliding surface and the super-twisting control law, the criterion for tuning the SMC-2 parameters is defined by positive values of λ and W. The PSO algorithm will optimize these values.

$$\begin{aligned} s(x)(-K_p(\frac{1}{L}(-\lambda|s|^{0.5} sign\,(s) - \int W sign\,(s) \\ -R_L i_d - v_d)) + K_i(i_d - i_{derf})) < 0 \end{aligned} \tag{21}$$

B. Controller's tunning

The following pseudocode shows the criterion for tuning the SMC-2. The search objective was the values of λ and W as seen in Table II.

C. Performance evaluation

To determine the effectiveness of the SMC-2, two performance indexes are proposed. The first one is the Integral of Absolute Error, and the other is the Integral of the Square Error [12].

$$IAE = \int_0^t |e\,(t)|\, dt \tag{22}$$

$$ISE = \int_0^t e(t)^2 dt \tag{23}$$

TABLE III
SWITCHING STATES OF POWER ELECTRONIC DEVICES ON SPVSI.

Simulation	SMC-2		PI	
	IAE	ISE	IAE	ISE
Active power ramp rates	0.127	0.762	0.130	0.845
Load consumption	0.223	207.4	0.265	209.88

IV. RESULTS

A. Active power transfer between SPVSI and the grid

The active power transfer between SPVSI and the grid is disposed of by the policy [13]. The value of the ramp is determined in 20% per minute of the maximum active power available. The value of the active power ramp is calculated as the battery bank voltage, and the electric charge is $V_{bat} = 400V$ and $Ih_{bat} = 100Ah$. Thus, the total active power available is $P_{tot} = 40000W = 40kW$, where the rate of the active ramp is defined as:

$$r_r = 0.2P_{tot}\frac{W}{min} = 8000\frac{W}{min} = 133.33\frac{W}{s} \quad (24)$$

A conventional PI regulator is added to this simulation to contrast the performance of SMC-2.

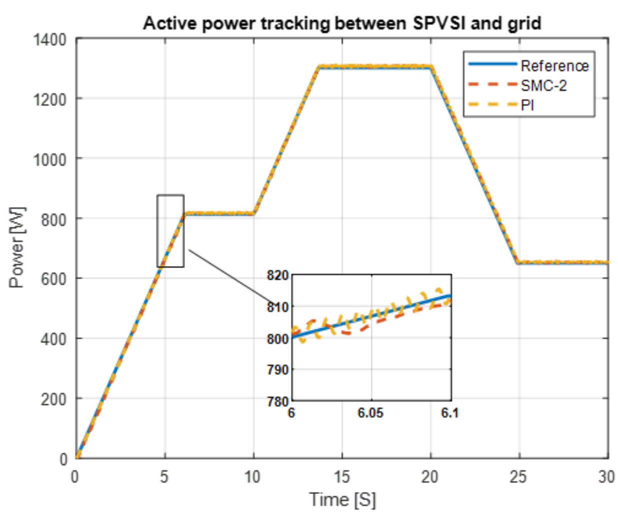

Fig. 3. Active power rate tracking.

The SMC-2 tunned by PSO follows better the ramp setpoint than PI controller. Oscillations in SMC-2 are less prominent than those generated by PI. The rate ramp value is set in watts per second for producing/receiving energy from the SPVSI.

A load is placed between the SPVSI and the grid to evaluate the performance of each controller. The results show the reference tracking value represented by the load. This value is taken from a load profile of a home of low-voltage consumption. The load data represent appliances like fridges, induction cooks, heaters, among others.

The standard of IEEE Std 1547-2018 requires inverter-based MGs voltage to be kept in a range of operations. The SPVSI in this experiment is recognized as Category A related to

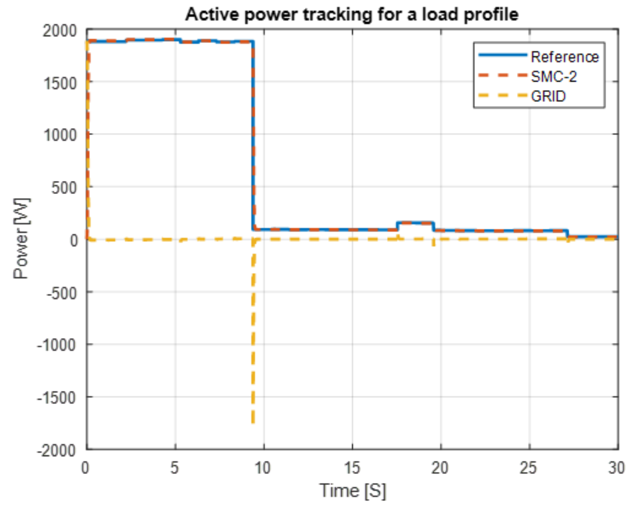

Fig. 4. Load profile for SMC-2 controller.

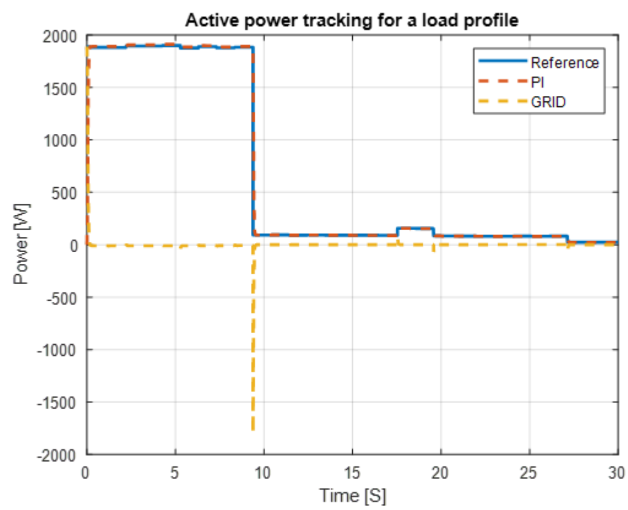

Fig. 5. Load profile for PI controller.

reactive power capability and voltage regulation. The proposed system covers the minimum performance capabilities needed for the Electric Power Systems area where the DG resources are lower.

The V_{rms} value can oscillate between $0.95V_N$ and $1.05V_N$, where V_N is 230V. The results show a proper control of the generated voltage by the SPVSI where the values do not reach the minimum and maximum limits of the policy. The maximum reached value is 232.9V.

From the point of view of abnormal performance categories, the IEEE Std 1547-2018 located in Category I to all installations covering minimal bulk power systems. The reliability is attainable to all distributed resources that are in common use.

The value of $0.5Hz$ is placed as the maximum and minimum limit for inverter-based MG operation. The DQ algorithm synchronizes to grid frequency in less than 1 s. Besides the ramp active power references, the SPVSI maintains the

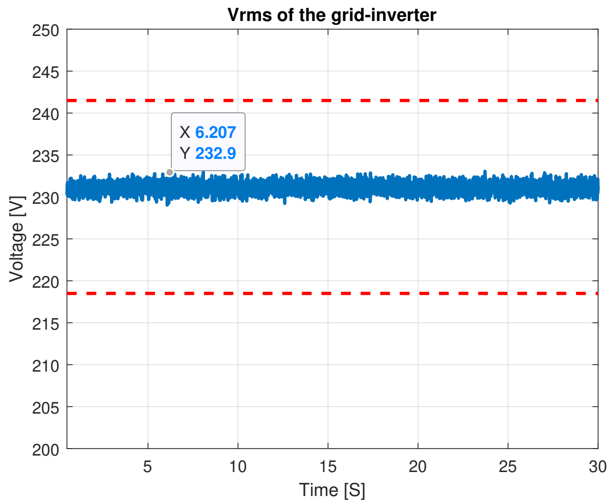

Fig. 6. Vrms on the grid for SMC-2 controller.

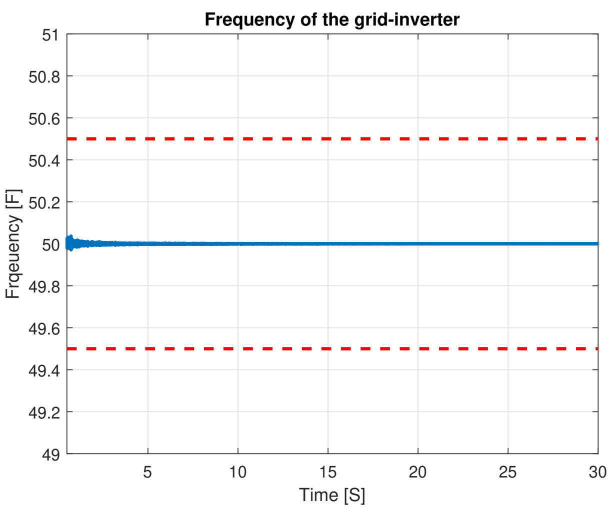

Fig. 7. Frequency on the grid for SMC-2 controller.

frequency in 50 Hz. Therefore, the small variations do not represent a significant disturbance that may lead to instability.

V. Conclusions

This paper presented the design and implementation of an SMC-2 for an SPVSI connected to the grid. The active power is produced and received in the SPVSI based on electrical policies when connected to the grid.

The SMC-2 used the super-twisting algorithm to avoid chartering effect without decreasing the robustness of the algorithm. The performance indexes used for this work (IAE and ISE) showed the best achievement of objectives of SMC-2. In addition, results on-ramp reference tracking showed precise control without damping and oscillations.

In addition, the tracking of references values of active power showed the compliment of stability values of voltage and frequency under the policy IEEE Std 1547-2018. The results demonstrated stable operation values for voltage and frequency without surpassing their upper and lower limits, respectively. These actions are uncovered by advanced algorithms yet in the field of smart inverters.

The SMC-2 dealt with the coupled model of the SPVSI in the DQ reference frame. The robustness of the SMC-2 surpasses the model uncertainties presented by elements like parasite capacitance on the SPVSI.

Due to the different obstacles to tuning a control algorithm, the PSO method is suitable for finding the controller's parameters. However, the PSO is a metaheuristics algorithm that consumes a high value of computational cost. The procedure followed in this work developed the greater cost computational algorithm separately in MATLAB™ to give the control law's parameters to the main simulation is PSCAD™.

Acknowledgment

This paper belongs to the project IEA.JCG.20.01 from Universidad de las Américas-Ecuador.

References

[1] J. Y. Lee, R. Verayiah, K. H. Ong, A. K. Ramasamy, and M. B. Marsadek, "Distributed generation: A review on current energy status, grid-interconnected pq issues, and implementation constraints of dg in malaysia," *Energies*, vol. 13, no. 24, 2020. [Online]. Available: https://www.mdpi.com/1996-1073/13/24/6479

[2] W. Shi, N. Li, C.-C. Chu, and R. Gadh, "Real-time energy management in microgrids," *IEEE Transactions on Smart Grid*, vol. 8, no. 1, pp. 228–238, 2017.

[3] J. Xu, Q. Qian, B. Zhang, and S. Xie, "Harmonics and stability analysis of single-phase grid-connected inverters in distributed power generation systems considering phase-locked loop impact," *IEEE Transactions on Sustainable Energy*, vol. 10, no. 3, pp. 1470–1480, July 2019.

[4] B. Sujatha and G. Anitha, "Grid synchronisation of photovoltaic distributed generation using hybrid fuzzy-pi controller."

[5] M. Babaie, M. Mehrasa, M. Sharifzadeh, G. Melis, and K. Al-Haddad, "Dq-based radial basis function controller for single-phase pec9 inverter," in *2020 IEEE 29th International Symposium on Industrial Electronics (ISIE)*, June 2020, pp. 701–706.

[6] F. Toso, A. Favato, R. Torchio, P. Alotto, and S. Bolognani, "Continuous control set model predictive current control of a microgrid-connected pwm inverter," *IEEE Transactions on Power Systems*, vol. 36, no. 1, pp. 415–425, Jan 2021.

[7] G. Bartolini, L. Fridman, A. Pisano, and E. Usai, *Modern sliding mode control theory: New perspectives and applications*. Springer, 2008, vol. 375.

[8] Z. Zhao, H. Gu, J. Zhang, and G. Ding, "Terminal sliding mode control based on super-twisting algorithm," *Journal of Systems Engineering and Electronics*, vol. 28, no. 1, pp. 145–150, Feb 2017.

[9] S. Nanchian, A. Majumdar, and B. C. Pal, "Three-phase state estimation using hybrid particle swarm optimization," *IEEE Transactions on Smart Grid*, vol. 8, no. 3, pp. 1035–1045, May 2017.

[10] J. H. Lee, J.-Y. Song, D.-W. Kim, J.-W. Kim, Y.-J. Kim, and S.-Y. Jung, "Particle swarm optimization algorithm with intelligent particle number control for optimal design of electric machines," *IEEE Transactions on Industrial Electronics*, vol. 65, no. 2, pp. 1791–1798, Feb 2018.

[11] S. Chaturvedi, D. Fulwani, and J. M. Guerrero, "Adaptive-smc based output impedance shaping in dc microgrids affected by inverter loads," *IEEE Transactions on Sustainable Energy*, vol. 11, no. 4, pp. 2940–2949, Oct 2020.

[12] A. S. Huaman Loayza and C. G. Pérez Zuñiga, "Design of a fuzzy sliding mode controller for the autonomous path-following of a quadrotor," *IEEE Latin America Transactions*, vol. 17, no. 06, pp. 962–971, June 2019.

[13] D. M. Rosewater, J. T. Johnson, M. Verga, R. Lazzari, C. Messner, and J. Hashimoto, "Sirfn draft test protocols for advanced battery energy storage system interoperability functions." Sandia National Lab.(SNL-NM), Albuquerque, NM (United States), Tech. Rep., 2016.